A systematic study on the effect of noise and shift on multivariate figures of merit of second-order calibration algorithms

Mohammad Ahmadvand [a], Hadi Parastar [b, *], Hassan Sereshti [a], Alejandro Olivieri [c], Roma Tauler [d]

[a] Department of Chemistry, Faculty of Science, University of Tehran, Tehran, Iran
[b] Department of Chemistry, Sharif University of Technology, P.O. Box 11155-3516, Tehran, Iran
[c] Departamento de Quimica Analitica, Facultad de Ciencias Bioquimicas y Farmacéuticas, Universidad Nacional de Rosario, Suipacha 531, 2000 Rosario, Argentina
[d] Institute of Environmental Assessment and Water Research, Spanish Council of Research, Jordi Girona 18, 08034 Barcelona, Spain

HIGHLIGHTS

- Development of multivariate AFOMs for hyphenated chromatographic measurements.
- Comparing the performance of MCR-ALS, PARAFAC and PARAFAC2 with multivariate AFOMs.
- Studying the effects of elution time shifts, noise, and interferences on AFOMs.
- Outperformance of MCR-ALS over PARAFAC and PARAFAC2 in terms of multivariate AFOMs.

GRAPHICAL ABSTRACT
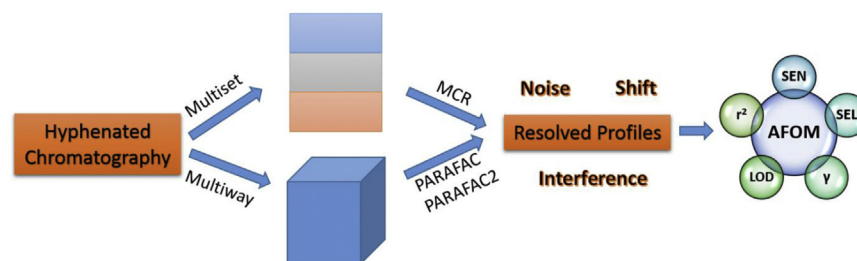
ABSTRACT

In the present study, multivariate analytical figures of merit (AFOM) for three well-known second-order calibration algorithms, parallel factor analysis (PARAFAC), PARAFAC2 and multivariate curve resolution-alternating least squares (MCR-ALS), were investigated in simulated hyphenated chromatographic systems including different artifacts (e.g., noise and peak shifts). Different two- and three-component systems with interferences were simulated. Resolved profiles from the target components were used to build calibration curves and to calculate the multivariate AFOMs, sensitivity (SEN), analytical sensitivity (γ), selectivity (SEL) and limit of detection (LOD). The obtained AFOMs for different simulated data sets using different algorithms were used to compare the performance of the algorithms and their calibration ability. Furthermore, phenanthrene and anthracene were analyzed by GC-MS in a mixture of polycyclic aromatic hydrocarbons (PAHs) to confirm the applicability of multivariate AFOMs in real samples. It is concluded that the MCR-ALS method provided the best resolution performance among the tested methods and that more reliable AFOMs were obtained with this method for the studied chromatographic systems with various levels of noise, elution time shifts and presence of unknown interferences.

© 2016 Elsevier B.V. All rights reserved.

1. Introduction

Undoubtedly, definition of analytical figures of merit (AFOM) is a powerful criterion for the evaluation and comparison of the

* Corresponding author.
E-mail addresses: h.parastar@sharif.edu, h.parastar@gmail.com (H. Parastar).

performance of analytical methods. Hence, having a precise calibration model and a uniform definition of AFOM are necessary tools for the comparison of analytical methods. On this matter, AFOM values for classical univariate calibration (i.e., zeroth-order calibration), where the signal should be sufficiently selective for the analyte of interest, are well defined and have been frequently discussed in the literature [1,2]. However, there are always still fundamental challenges for univariate calibration of systems without selectivity for the target analyte(s).

Recent advances in analytical instrumentation and the huge generation of data provided, have consequently brought the application of chemometric techniques able to extract useful and interpretable analytical information. Great efforts have been made to develop different multivariate calibration algorithms [3,4]. Since univariate AFOM definitions fail to describe the advances in this area, different approaches have been tried to redefine appropriate AFOMs according to multivariate calibration methods. The net analyte signal (NAS) concept for first-order calibration methods (like principal component regression (PCR) and partial least-squares (PLS)) has been reported by Lorber et al. [5] and then Ferre et al. [6]. However, for higher-order calibration methods, the NAS concept faces problems, such as diversity of definitions (like HCD defined by Ho, Christian, and Davidson [7], MKL defined by Messick, Kalivas, and Lang [8] and even a more general definition FO [9]) and also the difficulty in providing interpretable graphical results. On the other hand, a new sensitivity (SEN) definition has been developed according to the uncertainty propagation concept and it has been proposed for different multi-way decomposition algorithms, such as parallel factor analysis (PARAFAC), PLS coupled to residual multilinearization (PLS/RML) and multivariate curve resolution-alternating least squares (MCR-ALS) [10—12].

The latest development in this direction has been devoted to the definition of a unified sensitivity expression (SEN) for different calibration algorithms [13]. In this new definition, SEN is analyte specific, sample specific and algorithm specific. In fact, the SEN is calculated based on the amount of uncertainty in the test sample signal that it is propagated to concentration uncertainty. Other multivariate AFOMs, such as analytical sensitivity (γ), selectivity (SEL), limit of detection (LOD) and uncertainty in predicted concentration have been defined based on this SEN definition. It should be pointed out that the instrumental noise obtained for test samples is one of the most important parameters in the new SEN definition. In other words, this definition is reliable only when the instrumental noise is within acceptable limits. This definition has been successfully used in some studies with different decomposition algorithms [14—18]. Knowing the uncertainty limits in the output of instruments (uncertainty in signal) is strongly required for the employment of the proposed SEN definition in real samples analysis; under such circumstances, this definition is able to give acceptable AFOM values.

Nowadays, second-order calibration algorithms play an important role in accurate and precise analysis of excitation-emission spectroscopic systems and their use has been extended also to hyphenated chromatographic systems [19,20]. Different algorithms have been compared based on their ability to resolve the underlying components from different instrumental systems [21—24], but there is no report on the comparison of these algorithms related to the new SEN definition. Also, to the best of our knowledge, there is no report on the application of multivariate AFOM for hyphenated chromatographic systems. For this reason, there still remains work to be done to answer the relevant question regarding the method or algorithm specificity of the SEN definition: which method or algorithm may be applicable to instrumental data? Moreover, the effects on multivariate AFOM of chromatographic elution time shifts, of noise levels, and of presence/absence of

uncalibrated component(s) in the test set have not yet been studied.

In this research, the effects of elution time shift and noise levels on the performance of three frequently used second-order calibration algorithms (PARAFAC, PARAFAC2 and MCR-ALS) have been investigated. Multivariate analytical figures of merit, AFOM values, in hyphenated chromatographic systems were calculated, and their relation with bilinear (MCR-ALS) and trilinear (PARAFAC) data structures were evaluated. In addition, the effect of the number of components and the presence or absence of uncalibrated component(s) on algorithm performance, on the calibration model and on AFOM values were studied.

Several important facts should be noticed in this regard, which make our manuscript necessary.

(1) Still some researchers are applying PARAFAC to process chromatographic (either using uni- or bi-dimensional/multivariate detection) data. The fact that they were successful means that peak position and shape changes among different chromatographic runs did not occur or that they were minimal. However, this is often not the case and they were not checked, giving the (wrong) impression to readers that PARAFAC was applicable to this kind of data. This is the first aspect we wanted to reinforce in our paper, which is not generally accepted yet.

(2) The obvious sequel to PARAFAC, when chromatographic changes indeed occur, is PARAFAC2, which has been developed to cope with the chromatographic changes described in our manuscript. However, it is shown that PARAFAC2 cannot cope with them when they are strong, especially in cases where these changes in chromatographic peaks occur in the presence of un-calibrated interferences in test samples. Again, this is not universally appreciated. Researchers applying PARAFAC2 may find that the latter is applicable in cases where chromatographic changes are small and interferences are absent in test samples, but this is not the general situation. And this is the second reason why our manuscript is necessary.

(3) We think that the best model to cope with hyphenated chromatographic (uni-and multidimensional) data is the bilinear model as it is used in the MCR-ALS method. Perhaps this is not obvious to all researchers in the field, but the reason is simple: the bilinear MCR-ALS model is the model that properly fits the measured signal which linear with respect to the mixture of components weighted by their respective concentrations. This is finally the third important reason to support our manuscript.

2. Experimental

2.1. Simulated data

In order to evaluate the effects of shift and noise on multivariate AFOM values, three different hyphenated chromatographic systems were investigated:

(i) Two-component calibration system
(ii) Three-component calibration system
(iii) Two-component calibration system with two interferences in the test set

In these three systems, the number of elution times in the chromatographic mode was 100 and all mass spectra were simulated in a mass-to-charge (m/z) range 50—350 with intensities

between 0 and 1. To better emulate real situations, the mass spectra of some polycyclic aromatic hydrocarbons (PAHs) (i.e., biphenyl, fluorene, benzo[a]pyrene, pyrene) taken from the NIST library were used for this purpose. The elution profiles were simulated using an exponentially modified Gaussian (EMG) equation [25]. The EMG equation is defined as follows:

$$F(t) = \frac{h.\sigma}{\tau}\sqrt{\frac{\pi}{2}} \cdot e^{\left(\frac{\sigma^2}{2\tau^2} - \frac{t-\mu}{\tau}\right)} \cdot \left(1 - \text{erf}\left(\frac{1}{\sqrt{2}}\left(\frac{\mu - t}{\sigma} + \frac{\sigma}{\tau}\right)\right)\right) \quad (1)$$

where t is the elution time, h is the Gaussian height, σ is the Gaussian sigma, μ is the position of the unmodified Gaussian function, τ is the relaxation time parameter to modify the Gaussian function and erf is as follows:

$$\text{erf}(z) = \frac{2}{\sqrt{\pi}} \int_0^z e^{-t^2} dt \quad (2)$$

Fig. 1 shows the simulated elution and spectral profiles for the three simulated data sets. As can be seen from Fig. 1, different degrees of overlap were considered in different systems. For example, the degree of overlap in system (i) is lower than in systems (ii) and (iii).

The simulated elution profiles, C, have dimension of ($I \times N$) and mass spectral profiles, S, have dimension of ($J \times N$), where, I, J and N are the number of elution time points, spectral variables and number of chemical components, respectively. The hyphenated chromatographic data matrices with dimension ($I \times J$) were obtained by multiplying elution and spectral profiles, $\mathbf{CS}^T$.

In the next step, peak shifts were applied to these simulated elution profiles. Different shift levels were considered in each simulated system. As an example, the shift design for the simulated system (ii) is depicted in Table 1. Positive, null and negative signs are used to show different time shift scenarios to the right, no shifts and to the left, respectively. This design was followed in all cases (i.e., with shift levels of 1%, 3%, 5% and 10%). Fig. 2 shows the simulated profiles of system (ii) after application of different shift levels.

Homoscedastic noise (i.e., normally distributed noise) was then added to the data matrix with mean zero and standard deviation equal to 0.1%, 0.5% and 1% of the maximum intensity value in the data. Summarizing, from the combination of the different time shift and noise levels, 20 simulated data matrices were finally generated for each data system (i, ii and iii). These data sets were subsequently analyzed using the three different second-order calibration algorithms.

2.2. Experimental data

Calculation of AFOMs in a real experimental case is shown for a data set obtained in the GC-MS analysis of anthracene and phenanthrene in a standard mixture (Dr Ehrenstorfer, Augsburg, Germany) of polycyclic aromatic hydrocarbons (PAHs). This experimental data set is rather simple and it is mostly used here to illustrate how AFOMs can be evaluated for a real data case. Three sample replicates at seven concentration levels (0.02, 0.20, 0.50, 1.00, 2.00 4.00 and 5.00 mg L^{-1}) of anthracene and phenanthrene were analyzed. Analyses were performed with an Agilent 6890 GC system coupled to a 5973 network mass selective detector (Agilent Technologies, Santa Clara, CA, USA). The GC column consisted of TRB-5MS coated with 5% diphenyl, 95% dimethylpolysiloxane from Teknokroma (Sant Cugat del Vallès, Spain) (20 m × 0.18-mm inner diameter × 0.18-μm film thickness). The oven temperature was held at 65 °C for 1 min, ramped at 10 °C min^{-1} to 315 °C, and kept for 3 min. Mass spectra were taken at 70 eV ionization energy and in full scan mode. The scanned mass range was set at 50–350 m/z. In addition, 1.0 μL of each sample was injected in splitless injection mode.

2.3. Multiset and multiway arrangement of hyphenated chromatographic data sets

Hyphenated chromatographic systems generate multivariate data. GC-MS, LC-MS and LC-DAD are examples of hyphenated chromatographic systems that generate second-order data (i.e., containing two different types of instrumental variables like elution time points and wavelength in HPLC-DAD) for each analyzed sample. These generated data are usually nontrilinear due to the presence of changes in both elution times and peak shapes from sample to sample [19]. Losses of trilinearity can be afforded using different strategies, such as the application of peak alignment methods [26,27] before the application of the trilinear models (e.g., PARAFAC) [28] in some cases or by direct data analysis with algorithms such as MCR-ALS [29] and PARAFAC2 [30].

Depending on the type of second-order calibration algorithm, different types of data arrangement (i.e., multi-set matrix augmentation or multi-way tensors) are possible for hyphenated chromatographic data. For each sample, a data matrix is obtained which has i elution times and j spectral variables or wavelengths. In the analysis of k different samples (or chromatographic runs), multiple data matrices will be obtained. In PARAFAC and PARAFAC2, the k individual matrices ($I \times J$) are arranged in three-way, data cube, format $I \times J \times K$. In the case of MCR-ALS, the arrangement of multiple data matrices is performed using a column-wise augmented data matrix with dimension of $KI \times J$. In this arrangement, the bilinear model is maintained when the spectral mode (i.e., columns of augmented data matrix) is used as the common mode among the different data matrices) and the elution time mode is freely allowed to change for the different individual data matrices (i.e., rows of the augmented data matrix). This is in contrast to PARAFAC trilinear model, where the both modes, spectral and elution modes, should be common among the different data matrices considered and the data are arranged in a data cube. Differences among these approaches have been described in previous works [19,21–24].

2.4. Multivariate analytical figures of merit

Multivariate AFOMs were calculated according to ref. [13] where the sensitivity, SEN, is defined based on the estimated propagation of uncertainties. In this definition, the ratio of the uncertainty in the test sample signal to the uncertainty in the predicted concentration can be a good measure of SEN. According to this concept, the MCR-ALS sensitivity is defined as Eq. (3):

$$\text{SEN}_n = m_n \left[J(\mathbf{S}^T\mathbf{S})_{nn}^{-1}\right]^{-1/2} \quad (3)$$

where n is the index for the analyte of interest in a multi-component mixture, m_n is the slope of the MCR pseudo-univariate calibration graph for the target analyte (plot of the scores or relative concentrations of a given analyte vs. its nominal calibration concentrations), $\mathbf{S}^T$ is the matrix containing the profiles for all sample components in the non-augmented MCR direction, and J is the number of data points in the chromatographic direction of test sample. The readers are encouraged to consult ref. [12] for more details.

The PARAFAC SEN is estimated according to the expression:
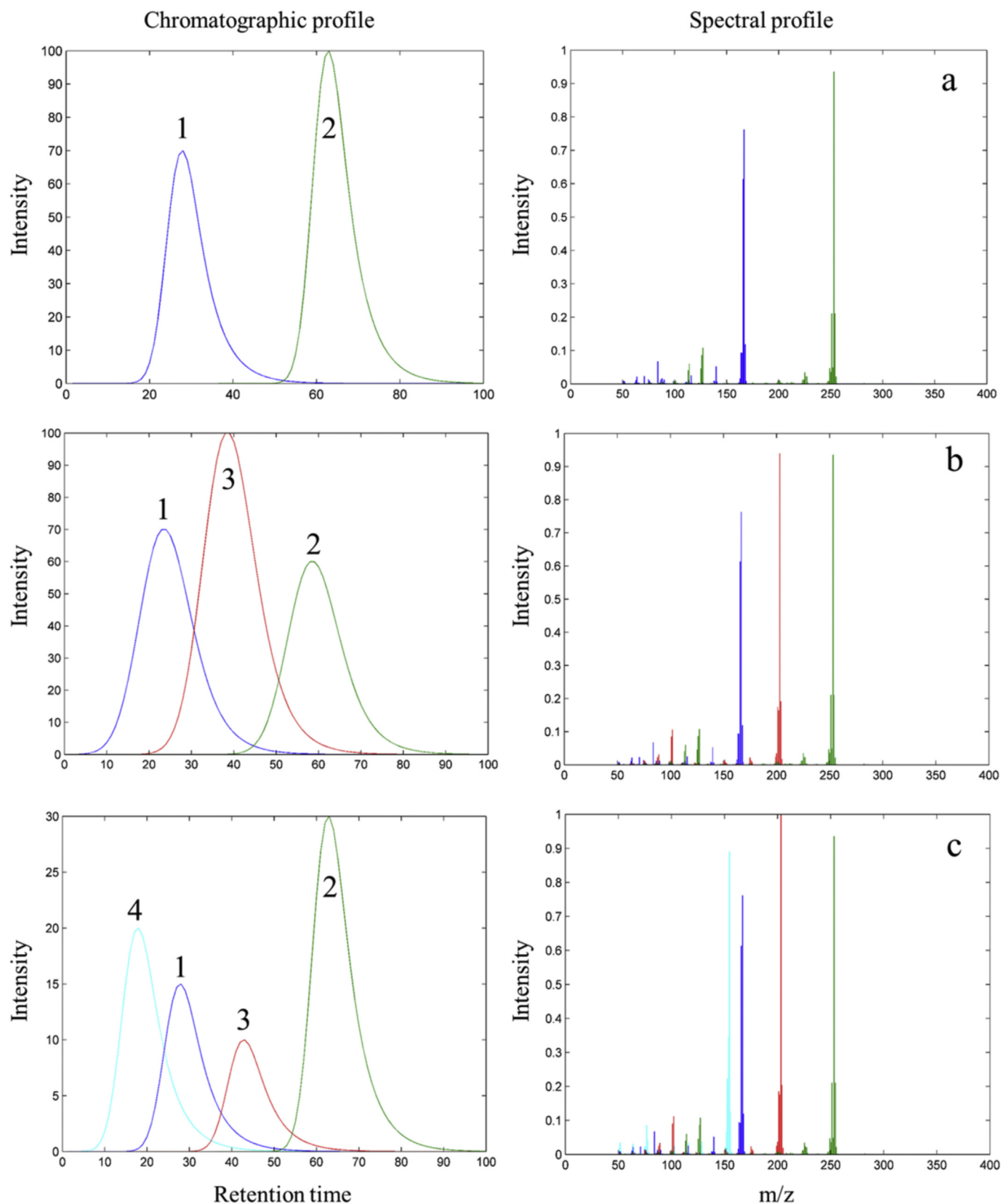
Fig. 1. Simulated chromatographic systems (*a*) system (*i*): calibrated two-component system, (b) system (*ii*): calibrated three-component system and (c) system (*iii*): calibrated two-component system with two uncalibrated components (i.e. 3 and 4) in the test set. Numbers refer to fluorene (green), benzo[*a*]pyrene (blue), pyrene (red) and biphenyl (cyan), respectively. (For interpretation of the references to colour in this figure legend, the reader is referred to the web version of this article.)

Table 1
The calibration levels and elution time shifts direction in system (*ii*).

Concentration level	Peak height			Replicate 1			Replicate 2			Replicate 3		
	C1	C2	C3	C1	C2	C3	C1	C2	C3	C1	C2	C3
100	70	100	60	0	−	−	+	+	+	0	+	0
50	35	50	30	+	0	+	−	+	−	0	+	+
10	7	10	6	−	−	+	0	−	0	+	−	+
5	3.5	5	3	−	0	−	+	−	−	−	−	0
1	0.7	1	0.6	0	0	−	+	+	−	+	0	0
0.5	0.35	0.5	0.3	+	+	0	0	0	+	−	+	+
0.1	0.07	1	0.06	0	0	0	−	0	0	−	−	−

The signs +, 0 and − show the shift to right, without shift and shift to left, respectively.

$$SEN_n = m_n \left\| \text{nth row of } \left[\left(I - \mathbf{Z}_{unx}\, \mathbf{Z}_{unx}{}^{+}\right) \mathbf{Z}_{exp} \right]^{+} \right\|^{-1} \tag{4}$$

where m_n is now the slope of PARAFAC pseudo-univariate calibration graph. Z_{exp} and Z_{unx} are defined according to Eqs. (5) and (6):

$$\mathbf{Z}_{exp} = m_n (\mathbf{C}_{exp} \odot \mathbf{B}_{exp}) \tag{5}$$

$$\mathbf{Z}_{unx} = [\mathbf{c}_1 \otimes \mathbf{I}_b | \mathbf{I}_c \otimes \mathbf{b}_1 | \mathbf{c}_2 \otimes \mathbf{I}_b | \mathbf{I}_c \otimes \mathbf{b}_2 |]\ldots \tag{6}$$

where $\mathbf{B}_{exp}$ and $\mathbf{C}_{exp}$ are respectively the elution and spectral loading matrices for the desired constituent(s) in the set of calibration samples. Profiles $\mathbf{b}_1$, $\mathbf{b}_2$ and $\mathbf{c}_1$, $\mathbf{c}_2$, are unexpected constituents in the elution and spectral modes, respectively. Also, $\mathbf{I}_b$ and $\mathbf{I}_c$ are identity matrices with appropriate dimensions, of size $J \times J$ and $K \times K$ respectively. Numbers 1, 2, …stand for the total number of unexpected constituents. The symbols $\odot$ and $\otimes$ indicate the Khatri-Rao and Kronecker products, respectively [31,32].

Other remaining AFOM values are defined based on SEN_n. The analytical sensitivity (γ_n) is defined as the ratio of the calibration SEN to the instrumental noise (σ_x). It is considered to be a better criterion to compare different analytical methods due to its independency from measured instrumental signal (Eq. (7)):

$$\gamma_n = SEN_n / \sigma_x \tag{7}$$

where σ_x is the signal uncertainty which can be calculated using the variance-covariance matrix of residuals [33]. It is important to remark that depending on the type of data arrangement used (i.e., matrix or cube) and on the data analysis (i.e., multi-set or multi-way) method, uncertainty in the signal can change.

SEL is one of the most important AFOMs which it has been rarely investigated in the literature. Despite its importance, there is no general expression for SEL yet. In this study, the SEL definition by Olivieri [34], as the ratio of mixture SEN (when all other sample constituents are present) to the considered analyte SEN, was used to calculate the SEL parameter. Selectivity, SEL, for MCR-ALS and PARAFAC were defined based on Eqs. (8) and (9), respectively:

$$SEL_n = SEN_n J^{1/2} \big/ m_n \tag{8}$$

$$SEL_n = SEN_n / m_n \tag{9}$$

Limit of detection (LOD) and limit of quantification (LOQ) are other AFOMs that can be defined based on the new SEN definition. In other words, LOD and LOQ are still defined based on false positive and false negative errors [13]. In this work, LOD and LOQ are defined as follows:

$$LOD_n = 3.3 \left(SEN_n^{-2} \sigma_x^2 + h_0 SEN_n^{-2} \sigma_x^2 + h_0 \sigma_{ycal}^2 \right)^{1/2} \tag{10}$$

$$LOD_n = 10 \left(SEN_n^{-2} \sigma_x^2 + h_0 SEN_n^{-2} \sigma_x^2 + h_0 \sigma_{ycal}^2 \right)^{\frac{1}{2}} \tag{11}$$

where SEN_n is the sensitivity calculated for the target analyte, σ_x^2 is the variance of the instrumental signals, σ_{ycal}^2 is the variance in the calibration concentrations and h_0 is the leverage for the blank sample.
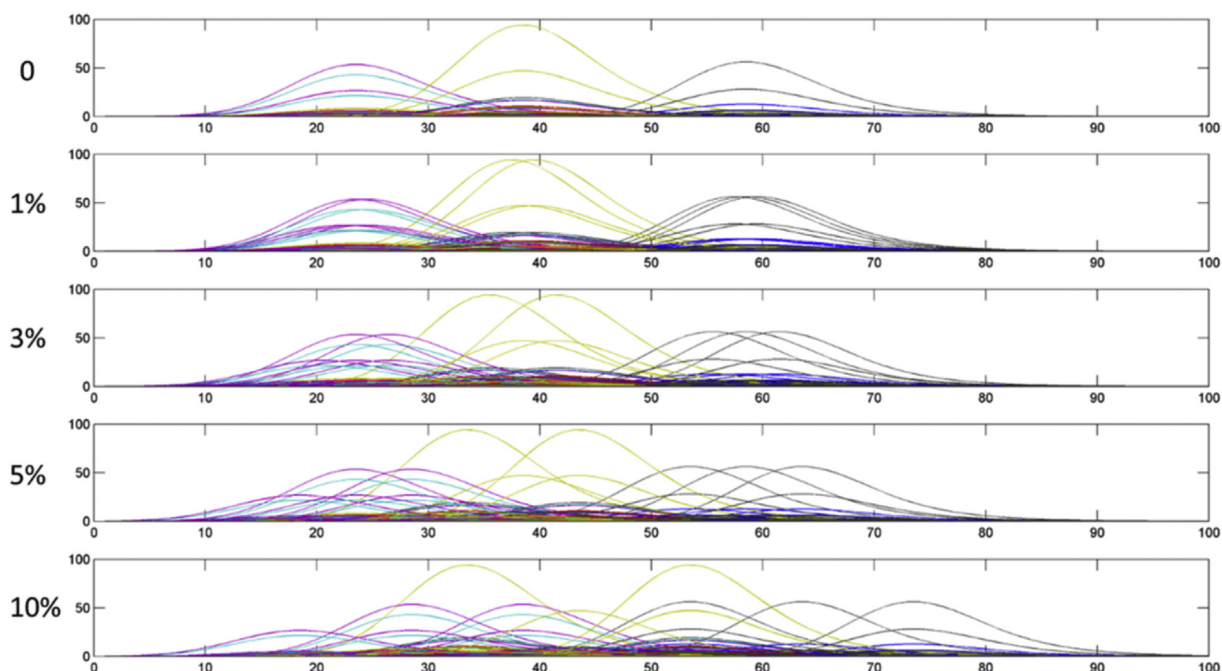
Fig. 2. Row-wise augmented data matrix of system (*ii*) at different elution time shift levels (0–10%).
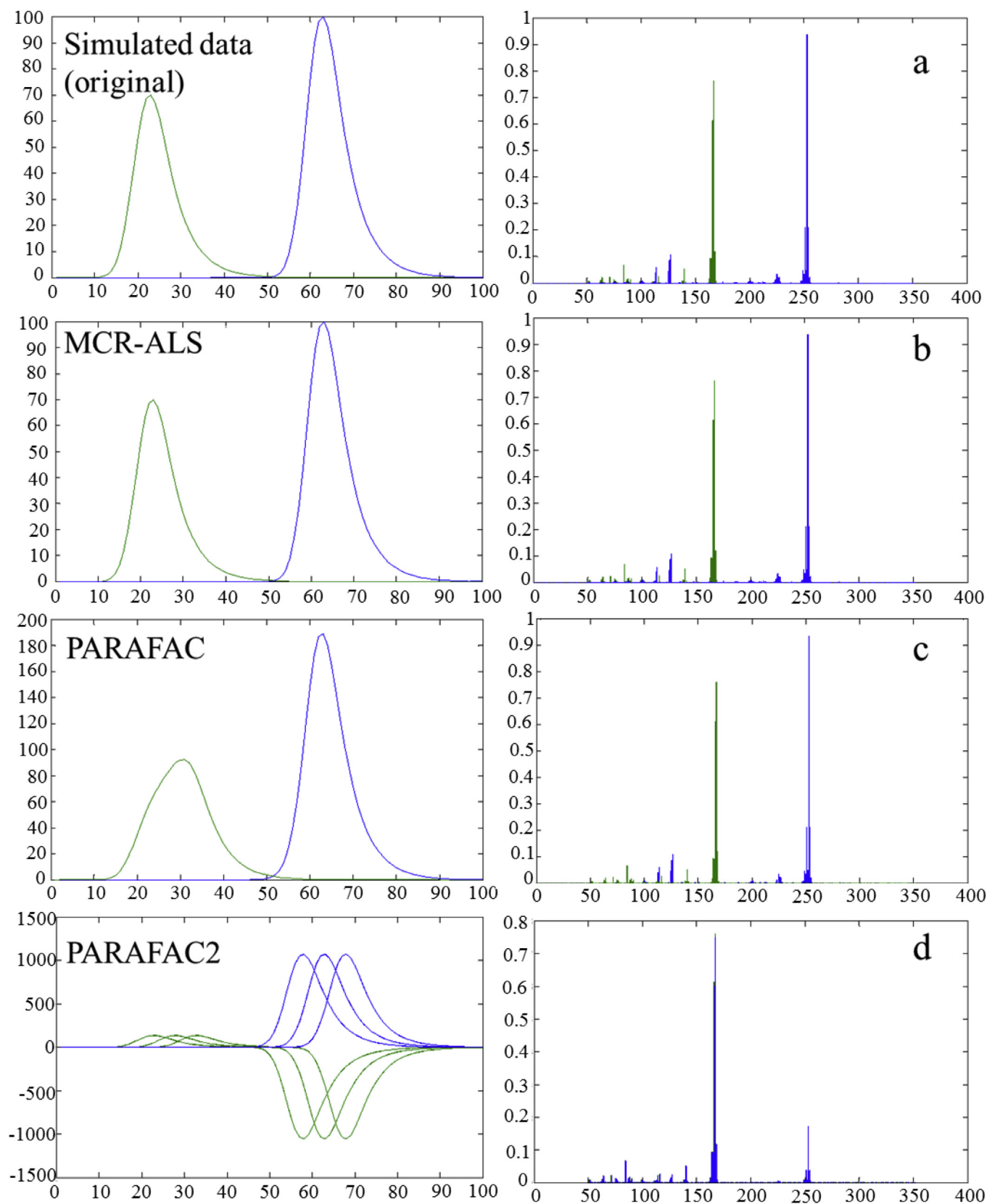
Fig. 3. Elution and spectral profiles of fluorene (green, left) and benzo[a]pyrene (blue, right) in (a) simulated data system (i) with 5% shift and 0.1% noise level, (b) resolved by MCR-ALS, (c) resolved by PARAFAC and (d) resolved by PARAFAC2. (For interpretation of the references to colour in this figure legend, the reader is referred to the web version of this article.)

2.5. Software

Data collection and exportation were done with an enhanced ChemStation software package (G1701 DA-MSD, Rev. D.00.01.27). Data were then exported in comma-separated value (CSV) format and imported into MATLAB version 2013Ra (The MathWorks, Natick, MA, USA). EMGPEAK MATLAB code was used for simulation of chromatographic profiles [25]. The spectral profiles (mass spectra) were given from NIST library [35]. The MCR-ALS and N-way version 3.1 toolboxes were used for MCR-ALS [36], PARAFAC and PARAFAC2 modeling [37]. Multivariate AFOMs were calculated based on ref. [13].

3. Results and discussion

The aim of this study was to investigate the effect of noise and shift on the performance of second-order calibration algorithms and also on their multivariate AFOMs. It has been discussed in previous works that resolving a nontrilinear data with a trilinear algorithm (i.e., PARAFAC) is not appropriate. However, it is important to show to which extent artifacts in the data can be tolerated by PARAFAC, and whether the results in terms of AFOMs are acceptable. In addition, a real GC-MS data set was also used to show how multivariate AFOMs can be calculated in these cases.

In brief, the operational conditions and constraints for the different algorithms were as follows:

— For MCR-ALS, the initial estimates were obtained using purest variable analysis [38] and different constraints, such as non-negativity (in both elution and spectral modes), unimodality (in elution mode), spectral normalization (to unit length) and component correspondence were applied during the ALS optimization.

— For PARAFAC, the initial estimates were obtained using random initialization, singular value decomposition (SVD) and solutions of 10 best initial PARAFAC runs. Also, non-negativity (in elution, spectral and concentration mode) and unimodality (in elution mode) constraints were applied during optimization.

— For PARAFAC2, the initial estimates were obtained using the SVD and solutions of 10 best initial PARAFAC2 runs and non-negativity constraints were applied in spectral and concentration modes (PARAFAC2 does not admit constraints in the elution time mode).

In the next sections, results of the analysis of the three simulated chromatographic systems with these different second-order calibration algorithms will be given, along with the results of the calculation of multivariate AFOMs in each case. For brevity, the results for two-component system (benzo[*a*]pyrene with a sharp peak at *m/z* 252 and fluorene with a sharp peak at *m/z* 166) with 5% random shift and 0.1% noise will be discussed in detail for the three simulated systems and also for one experimental system.

3.1. Two-component calibration system (i)

In this data system (i), there are seven concentration levels and three replicates, giving 21 individual matrices with dimension of 100×301. These individual matrices were then arranged in a single column-wise augmented data matrix of dimensions 2100×301 which was analyzed by MCR-ALS. In the case of PARAFAC and PARAFAC2, the 21 individual data matrices (data slices) were arranged in a three-way data array (data cube) with dimensions of $301 \times 100 \times 21$.

Fig. 3 shows the elution and spectral profiles resolved using MCR-ALS (Fig. 3b), PARAFAC (Fig. 3c) and PARAFAC2 (Fig. 3d) respectively, for data with a 5% of elution time shift and a 0.1% of noise. The corresponding profiles used in data simulation are given in Fig. 3a. As it can be seen, MCR-ALS could recover correctly both elution and spectral profiles. Elution profiles resolved by PARAFAC did not match the true profiles, although the resolved spectral profiles were well resolved. PARAFAC2 did not resolve correctly neither the elution nor the spectral profiles. PARTAFAC2 converged to a solution with unreliable profiles. This is probably due to the complex pattern of random shifts at different concentrations and replicates used in the data simulation, which caused PARAFAC2 cross products to be different from sample to sample. When this happens, PARAFAC2 cannot resolve elution and spectral profiles properly [24]. In other words, when elution time shifts are severe, then, the cross-product constraint of PARAFAC2 cannot be preserved and therefore, PARAFAC2 produces unreasonable results. This effect has been studied in detail in Ref. [24]. LOF values (see definition of LOF value in the footnote of Table 2) were 2.77 and 33.90 for MCR-ALS and PARAFAC respectively, confirming the better performance of MCR-ALS compared to PARAFAC. Since LOF values depend on the data residual values, i.e., when the residual matrix as small values, LOF values will be low. When a resolution algorithm correctly recovers the components of the system and their profiles, LOF will be close to the standard deviation of the noise in the experimental data.

Finally, MCR-ALS resolved elution profiles were used to build calibration curves and to calculate the AFOM values. The calibration regression coefficient (r^2) of the calibration curve and relative error (RE, %) for the first component (benzo [a] pyrene; blue profiles in Fig. 3) were respectively 1.0000 and 2.90×10^{-3} for MCR-ALS and 0.9982 and 3.51 for PARAFAC. Furthermore, the r^2 and RE values for the second component (fluorene; green profiles in Fig. 3) for MCR-ALS and PARAFAC were respectively, 1.0000, 1.52×10^{-2} and 0.9995, 1.85. Pseudo-univariate calibration parameters already showed that MCR-ALS had probably a better performance than PARAFAC. Using the resolved spectral profiles and calibration parameters (e.g., slope of pseudo-univariate calibration, predicted concentration, number of calibration points, initial concentration and obtained signal), multivariate AFOMs were calculated. γ_n, SEL and LOD for the first component (benzo [a] pyrene) resolved by MCR-ALS were 3.80×10^1, 1.00 and 9.45×10^{-2}, respectively. γ_n, SEL and LOD for the first component resolved by PARAFAC were 9.00×10^{-2}, 1.00 and 3.93×10^1, respectively. For the second component (fluorene), γ_n, SEL and LOD for MCR-ALS were 2.70×10^1, 1.00 and 1.36×10^{-1} respectively while these parameters were 6.00×10^{-4}, 1.00 and 5.68×10^1 for PARAFAC. Tables 2 and 3 summarize these results for the two resolved components of data set (*i*). Also, in the footnote of this Table, the definitions of LOF and RE are given. It is concluded that the obtained PARAFAC calibration model was not given correct results for this simulated data set, with a poor calibration performance in terms of multivariate AFOMs compared to MCR-ALS algorithm.

In the case of PARAFAC2, reliable spectral and elution profiles were obtained only in the case of noiseless data sets. Only in these cases, results from PARAFAC2 were better than those from PARAFAC, and they were similar to those from MCR-ALS. LOF values were in the range of $1.30 \times 10^{-7} - 1.43$ for 0–10% elution time shift levels. For instance, the multivariate AFOMs for PARAFAC2 in noiseless data were in the range γ_n between $3.70 \times 10^{15} - 2.20 \times 10^1$, SEL = 1.00 and LOD between $1.12 \times 10^{-8} - 1.67 \times 10^{-1}$ for fluorene at elution time shift levels 0–10%.

Final results (calibration parameters and multivariate AFOMs) for fluorene in system (*i*) are presented in Tables 4 and 5. As it can be seen, the results at all elution time shift and noise levels showed the same trend as those discussed in previous example. Results (calibration parameters and multivariate AFOMs) for all investigated elution time shifts and noise levels for benzo [a] pyrene are

Table 2
Benzo[*a*]pyrene results with a 5% elution shift and a 0.1% noise level.

	LOF[a]	r^{2}[b]	RE[c]	γ[d]	SEL[e]	LOD[f]
System (i)						
MCR-ALS	2.77	1.0000	2.90×10^{-3}	3.80×10^{1}	1.00	9.45×10^{-2}
PARAFAC	3.39×10^{1}	0.9982	3.51	9.00×10^{-2}	1.00	3.93×10^{1}
PARAFAC2	2.76	N.R[g]	N.R	N.R	N.R	N.R
System (ii)						
MCR-ALS	2.07	1.0000	7.50×10^{-3}	3.20×10^{1}	1.00	1.14×10^{-1}
PARAFAC	3.83×10^{1}	0.9997	1.33	3.10×10^{-2}	9.60×10^{-1}	1.20×10^{2}
PARAFAC2	2.23	N.R	N.R	N.R	N.R	N.R
System (iii)						
MCR-ALS	2.75	1.0000	4.00×10^{-3}	4.10×10^{1}	1.00	8.87×10^{-2}
PARAFAC	2.29×10^{1}	0.9983	3.45	1.20×10^{-1}	6.30×10^{-1}	3.14×10^{1}
PARAFAC2	2.91	1.0000	1.88×10^{-2}	2.80×10^{1}	6.00×10^{-1}	1.29×10^{-1}

[a] $Lack\ of\ fit(\%) = \sqrt{\sum_{ij} e_{ij}^{2} / \sum_{ij} x_{ij}^{2}} \times 100$, where x_{ij} and e_{ij} are the elements of the matrices X and E, respectively.

[b] Regression coefficient.

[c] $Relative\ error(\%) = (\sqrt{\sum_{i}(c_{i} - \hat{c}_{i})^{2}} / \sqrt{\sum_{i} c_{i}^{2}}) \times 100$, where c_{i} is the known concentration of standard i and $\hat{c}_{i}$ is its calculated value using the calibration equation obtained from the integrated peak area.

[d] Analytical sensitivity.

[e] Selectivity.

[f] Limit of detection calculated according to ref. [17].

[g] Not resolved because the reasonable profiles were not achieved.

presented in Tables S1 and S2 of supporting information (SI).

3.2. Three-component calibration system (ii)

System (*ii*) has three calibrated components. Overlapping degree in this system was higher than in system (*i*). Similar to previous example, results were presented for the special case of 5% of elution time shift and 0.1% of noise level. Fig. 4 shows elution and spectral profiles resolved by MCR-ALS (Fig. 4b), PARAFAC (Fig. 4c) and PARAFAC2 (Fig. 4d). Elution and spectral profiles used for data simulation are also shown for comparison in Fig. 4a. In this case, elution and spectral profiles were successfully recovered by MCR-ALS and PARAFAC. Again, PARAFAC2 could not resolve properly the pure component profiles (with 10000 iterations and 10^{-5} as stopping criterion). Since elution time shifts in this study were rather high, PARAFAC2 could not properly resolve the pure component profiles. As a consequence, negative values appeared in

the elution profiles, which resulted unreliable.

Similar to the previous case, LOF values of MCR-ALS models increased from 6.00×10^{-5} to 2.03×10^{1} when noise levels also increased from 0 to 1%, respectively (see Table S4). It is important to note that changes in LOF values were relatively independent of the shift level, which is a good confirmation of the flexibility of the bilinear MCR-ALS model. On the other hand, LOF values in PARAFAC models were dependent on elution time shift levels. For example, in noiseless cases, with increasing elution time shift levels from 0 to 10%, LOF% values changed from 5.00×10^{-5} to 4.84×10^{1} (Table S4). These changes of LOF values in noiseless data sets show the limitation of the trilinear PARAFAC model for cases with strong elution time shifts, like in the chromatographic data analyzed in this case. Other quantitative measures, such as r^2 and RE showed similar trends. RE values for MCR-ALS and PARAFAC were 7.50×10^{-3} and 1.33, respectively. Finally, the AFOMs for benzo [a] pyrene were calculated. The values of γ_n, SEL and LOD obtained with MCR-ALS

Table 3
Fluorene results with a 5% elution time shift and 0.1% noise level.

	LOF[a]	r^{2}[b]	RE[c]	γ[d]	SEL[e]	LOD[f]
System (i)						
MCR-ALS	2.77	1.0000	1.52×10^{-2}	2.70×10^{1}	1.00	1.36×10^{-1}
PARAFAC	3.39×10^{1}	0.9995	1.85	6.00×10^{-4}	1.00	5.68×10^{1}
PARAFAC2	2.76	N.R[g]	N.R	N.R	N.R	N.R
System (ii)						
MCR-ALS	2.07	1.0000	5.10×10^{-3}	3.70×10^{1}	1.00	9.90×10^{-2}
PARAFAC	3.83×10^{1}	0.9968	4.68	3.40×10^{-2}	9.60×10^{-1}	1.10×10^{2}
PARAFAC2	2.23	N.R	N.R	N.R	N.R	N.R
System (iii)						
MCR-ALS	2.75	1.0000	1.53×10^{-2}	2.90×10^{1}	1.00	1.30×10^{-1}
PARAFAC	2.29×10^{1}	0.9832	1.08×10^{1}	6.00×10^{-4}	9.00×10^{-3}	5.76×10^{3}
PARAFAC2	2.91	1.0000	4.05×10^{-1}	5.40×10^{-1}	1.60×10^{-2}	6.79

[a] $Lack\ of\ fit(\%) = \sqrt{\sum_{ij} e_{ij}^{2} / \sum_{ij} x_{ij}^{2}} \times 100$ where x_{ij} and e_{ij} are the elements of the matrices X and E, respectively.

[b] Regression coefficient.

[c] $Relative\ error(\%) = (\sqrt{\sum_{i}(c_{i} - \hat{c}_{i})^{2}} / \sqrt{\sum_{i} c_{i}^{2}}) \times 100$, where c_{i} is the known concentration of standard i and $\hat{c}_{i}$ is its calculated value using the calibration equation obtained from the integrated peak area.

[d] Analytical sensitivity.

[e] Selectivity.

[f] Limit of detection calculated according to ref. [17].

[g] Not resolved because the reasonable profiles were not achieved.

Table 4
Calibration parameters for fluorene in system (*i*).

Noise	Shift	Calibration equation						Regression coefficient (r^2)			Relative error (RE %)		
		Slope			Intercept								
		MCR-ALS	PARAFAC	PARAFAC2	MCR-ALS	PARAFAC	PARAFAC2	MCR-ALS	PARAFAC	PARAFAC2	MCR-ALS	PARAFAC	PARAFAC2
0	0	8.12	8.13	8.06	1.00×10^{-30}	6.00×10^{-13}	4.00×10^{-14}	1.0000	1.0000	1.0000	3.00×10^{-4}	1.00×10^{-8}	3.00×10^{-4}
	1%	8.12	8.12	8.06	4.00×10^{-4}	-1.49×10^{-2}	-3.00×10^{-5}	1.0000	1.0000	1.0000	2.00×10^{-4}	1.54×10^{-1}	4.00×10^{-4}
	3%	8.12	8.10	8.05	2.00×10^{-4}	-1.02×10^{-1}	-3.00×10^{-4}	1.0000	0.9998	1.0000	1.00×10^{-4}	1.09	6.00×10^{-4}
	5%	8.12	8.06	8.04	2.00×10^{-4}	-1.55×10^{-1}	-1.30×10^{-3}	1.0000	0.9995	1.0000	6.00×10^{-4}	1.86	1.90×10^{-3}
	10%	8.13	7.88	7.92	1.00×10^{-4}	3.89×10^{-1}	-5.30×10^{-2}	1.0000	0.9998	1.0000	3.00×10^{-4}	1.22	6.98×10^{-2}
0.1%	0	8.12	8.14	N.R	2.86×10^{-2}	7.80×10^{-3}	N.R	1.0000	1.0000	N.R	3.37×10^{-2}	7.00×10^{-3}	N.R
	1%	8.12	8.14	N.R	-2.20×10^{-2}	-2.90×10^{-2}	N.R	1.0000	1.0000	N.R	2.36×10^{-2}	1.67×10^{-1}	N.R
	3%	8.12	8.11	N.R	1.14×10^{-2}	-9.36×10^{-2}	N.R	1.0000	0.9998	N.R	6.40×10^{-2}	1.09	N.R
	5%	8.12	8.06	N.R	2.26×10^{-2}	-1.56×10^{-1}	N.R	1.0000	0.9995	N.R	1.52×10^{-2}	1.85	N.R
	10%	8.13	7.88	N.R	-2.43×10^{-2}	3.57×10^{-1}	N.R	1.0000	0.9998	N.R	1.66×10^{-2}	1.22	N.R
0.5%	0	8.12	8.15	N.R	-1.31×10^{-1}	6.00×10^{-13}	N.R	1.0000	1.0000	N.R	1.30×10^{-1}	1.04×10^{-1}	N.R
	1%	8.11	8.14	N.R	-5.75×10^{-2}	-1.49×10^{-2}	N.R	1.0000	1.0000	N.R	7.57×10^{-2}	1.45×10^{-1}	N.R
	3%	8.12	8.11	N.R	-4.75×10^{-2}	-1.02×10^{-1}	N.R	1.0000	0.9998	N.R	7.16×10^{-2}	1.10	N.R
	5%	8.14	8.09	N.R	-1.64×10^{-1}	-1.55×10^{-1}	N.R	1.0000	0.9995	N.R	1.70×10^{-1}	1.84	N.R
	10%	8.09	7.85	N.R	1.81×10^{-1}	3.89×10^{-1}	N.R	1.0000	0.9997	N.R	1.57×10^{-1}	1.34	N.R
1%	0	8.09	8.18	N.R	1.81×10^{-1}	7.80×10^{-3}	N.R	1.0000	1.0000	N.R	3.05×10^{-1}	8.49×10^{-2}	N.R
	1%	8.11	8.13	N.R	1.59×10^{-1}	-2.90×10^{-2}	N.R	1.0000	1.0000	N.R	1.39×10^{-1}	1.74×10^{-1}	N.R
	3%	8.14	8.14	N.R	-2.06×10^{-1}	-9.36×10^{-2}	N.R	1.0000	0.9998	N.R	1.35×10^{-1}	1.13	N.R
	5%	8.11	8.09	N.R	-9.37×10^{-2}	-1.56×10^{-1}	N.R	1.0000	0.9994	N.R	1.59×10^{-1}	2.00	N.R
	10%	8.12	7.84	N.R	-1.93×10^{-2}	3.57×10^{-1}	N.R	1.0000	0.9997	N.R	7.09×10^{-2}	1.37	N.R

were 3.20×10^1, 1.00 and 1.14×10^{-1} respectively, while they were 3.10×10^{-2}, 0.96 and 1.20×10^2 for PARAFAC (see Table 2). Table 3 shows calibration results and multivariate AFOMs obtained for fluorene for the investigated elution time shifts and noise levels (green profiles in Fig. 4).

The γ_n value obtained for MCR-ALS model for benzo [a] pyrene decreased from 8.70×10^9 to 3.20×10^{-1} when noise level increased from 0 to 1%. Also, LOD values for MCR-ALS increased from 3.39×10^{-9} to 1.15×10^1. For PARAFAC, a descending trend of γ_n was observed when both noise and elution time shift levels increased, which reflects a more complicated pattern. In this regard, the value of γ_n changed from 2.50×10^{10} to 1.30×10^{-2}. In accordance with the decrease of γ_n, LOD values increased from 1.50×10^{-10} to 2.90×10^2 (Table S8).

PARAFAC2 LOF values were rather similar to those from MCR-ALS. However, component profiles resolved by PARAFAC2 were not reasonable. Resolved elution profiles had negative values and

they were bimodal. Also, the resolved spectral profiles were wrongly overlapped. No PARAFAC2 results are finally given and they have been reported as not resolved (N.R.) in the tables. Results for fluorene, pyrene and benzo [a] pyrene of this system (at different elution time shifts and noise levels) are given in Table S3-S8.

3.3. Two-component calibration system with two-interferences in the test set (iii)

In the last simulated chromatographic system, the effect of interferences (absent in the calibration samples set but present in the test samples set) on calibration parameters and multivariate AFOMs was studied in more detail. For this purpose, two interferences were added to the test samples set, which heavily overlap with the two target analytes (see Fig. 1). Including the test data set (with three replicates) in the simultaneous analysis,

Table 5
Different algorithm performances and multivariate AFOM for fluorene in system (*i*).

| Noise	Shift	LOF %			SEL			γ			LOD		
		MCR-ALS	PARAFAC	PARAFAC2	MCR-ALS	PARAFAC	PARAFAC2	MCR-ALS	PARAFAC	PARAFAC2	MCR-ALS	PARAFAC	PARAFAC2
0	0	3.25×10^{-9}	4.00×10^{-5}	1.30×10^{-7}	1.00	1.00	1.00	4.20×10^{18}	4.70×10^{10}	2.60×10^{15}	3.99×10^{-9}	7.82×10^{-11}	1.63×10^{-11}
	1%	2.00×10^{-4}	8.56×10^1	2.21×10^{-2}	1.00	1.00	1.00	7.90×10^8	8.70×10^{-1}	1.10×10^5	1.12×10^{-4}	4.16	6.88×10^{-5}
	3%	1.00×10^{-4}	2.34×10^1	8.20×10^{-2}	1.00	1.00	1.00	2.10×10^9	1.20×10^{-1}	7.20×10^3	7.03×10^{-5}	2.93×10^1	6.21×10^{-1}
	5%	1.00×10^{-4}	3.38×10^1	1.94×10^{-1}	1.00	1.00	1.00	3.80×10^9	6.00×10^{-2}	1.10×10^3	5.51×10^{-5}	5.69×10^1	3.71×10^{-3}
	10%	2.82×10^{-5}	4.61×10^1	1.43	1.00	1.00	1.00	3.80×10^{10}	3.00×10^{-2}	1.50×10^1	3.45×10^{-5}	1.05×10^2	2.52×10^{-1}
0.1%	0	2.76	2.77	2.76	1.00	1.00	N.R	2.70×10^1	2.70×10^1	N.R	1.38×10^{-1}	1.35×10^{-1}	N.R
	1%	2.76	8.99×10^1	2.76	1.00	1.00	N.R	2.70×10^1	8.60×10^{-1}	N.R	1.36×10^{-1}	4.20	N.R
	3%	2.76	2.35×10^1	2.76	1.00	1.00	N.R	2.70×10^1	1.20×10^{-1}	N.R	1.35×10^{-1}	2.93×10^1	N.R
	5%	2.77	3.39×10^1	2.76	1.00	1.00	N.R	2.70×10^1	6.00×10^{-2}	N.R	1.36×10^{-1}	5.68×10^1	N.R
	10%	2.76	4.62×10^1	2.76	1.00	1.00	N.R	2.70×10^1	3.00×10^{-2}	N.R	1.35×10^{-1}	1.05×10^2	N.R
0.5%	0	1.37×10^1	1.37×10^1	1.36×10^1	1.00	1.00	N.R	1.10	1.10	N.R	3.35	3.34	N.R
	1%	1.37×10^1	1.62×10^1	1.37×10^1	1.00	1.00	N.R	1.10	6.10×10^{-1}	N.R	3.38	5.98	N.R
	3%	1.37×10^1	2.70×10^1	1.37×10^1	1.00	1.00	N.R	1.10	1.20×10^{-1}	N.R	3.38	3.04×10^1	N.R
	5%	1.37×10^1	3.61×10^1	1.37×10^1	1.00	1.00	N.R	1.10	6.00×10^{-2}	N.R	3.35	5.76×10^1	N.R
	10%	1.37×10^1	4.77×10^1	1.37×10^1	1.00	1.00	N.R	1.10	3.00×10^{-2}	N.R	3.38	1.07×10^2	N.R
1%	0	2.66×10^1	2.66×10^1	2.65×10^1	1.00	1.00	N.R	2.70×10^{-1}	2.70×10^{-1}	N.R	1.35×10^1	1.34×10^1	N.R
	1%	2.67×10^1	2.80×10^1	2.66×10^1	1.00	1.00	N.R	2.70×10^{-1}	2.40×10^{-1}	N.R	1.35×10^1	1.51×10^1	N.R
	3%	2.66×10^1	3.49×10^1	2.66×10^1	1.00	1.00	N.R	2.70×10^{-1}	1.00×10^{-1}	N.R	1.34×10^1	3.51×10^1	N.R
	5%	2.67×10^1	4.21×10^1	2.67×10^1	1.00	1.00	N.R	2.70×10^{-1}	6.00×10^{-2}	N.R	1.36×10^1	6.18×10^1	N.R
	10%	2.68×10^1	5.19×10^1	2.67×10^1	1.00	1.00	N.R	2.70×10^{-1}	3.00×10^{-2}	N.R	1.36×10^1	1.11×10^2	N.R
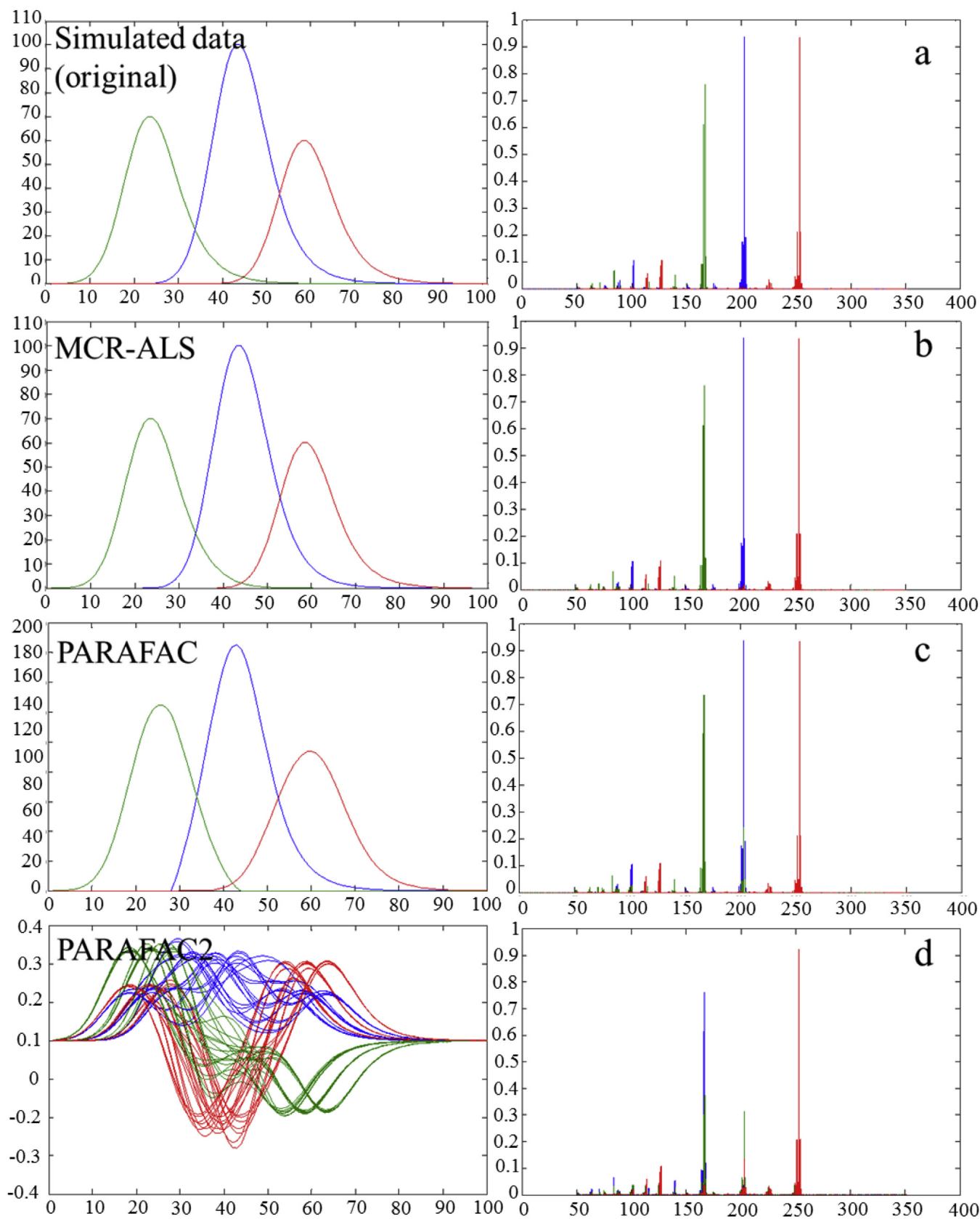
Fig. 4. Elution and spectral profiles of fluorene (green, left), pyrene (red, middle) and benzo[a]pyrene (blue, right) in (a) simulated data system (ii) with 5% shift and 0.1% noise level, (b) resolved by MCR-ALS, (c) resolved by PARAFAC and (d) resolved by PARAFAC2. (For interpretation of the references to colour in this figure legend, the reader is referred to the web version of this article.)

increased the dimensions of the augmented data matrices for MCR-ALS and three-way data arrays for PARAFAC and PARAFAC2 to $2400 \times 301, 100 \times 301 \times 24$ and $301 \times 100 \times 24$, respectively. In the two data systems previously examined, calibration samples and test samples had the same number of components, and only the effects of the elution time shift and of noise levels were examined. For comparison purposes, the data example with a 5% of time shift and a 0.1% of noise (without interferences) studied in previous sections was also discussed here. Fig. 5 shows the resolved profiles obtained by MCR-ALS (Fig. 5b), PARAFAC (Fig. 5c) and PARAFAC2 (Fig. 5d) methods. Component profiles used for the data simulation are shown in Fig. 5a. Only MCR-ALS was able to recover correctly the elution and spectral profiles of the two components. Due to the additional presence of uncalibrated interferences apart from increasing elution time shifts and noise levels, PARAFAC and PARAFAC2 methods could not resolve reliable profiles (see the values of SEL, γ and LOD in Tables S10 and S12). In addition, PARAFAC2 had again the problem of negative values in second mode elution profiles of the components in the test samples. As it has mentioned earlier, this is again due to the impossibility of the fulfillment of the cross-product constraint among different samples, because of the severe elution time shifts and/or interferences.

Results for the flourene and benzo [a] pyrene mixtures (*iii*) are shown in Tables 2 and 3. As it can be seen in these tables, there were no significant differences between the MCR-ALS results in absence or presence of interferences. For PARAFAC, LOF for system (*iii*) was 22.9 in contrast to 33.9 for system (*i*), which shows the unequal behavior of PARAFAC when uncalibrated species are present. PARAFAC results, for benzo [a] pyrene in system (*iii*) were similar to those for system (*i*), but flourene was more poorly resolved in system (*iii*) than in system (*i*). These worse results are also confirmed in Fig. 5, where spectral profiles of calibrated and uncalibrated species were not properly resolved by PARAFAC. Calibration parameters and multivariate AFOMs for system (*iii*) at different elution time shifts and noise levels are given in Table S9-S12.

3.4. Real GC-MS data

To check the applicability of multivariate AFOMs in the case of experimental data, a real GC-MS data set from the GC-MS analysis of standard mixture of PAHs was also evaluated for the quantitation of phenanthrene and anthracene in PAH mixtures. The data arrangement and analysis were carried out in a similar way to how it was performed for simulated data (section 2.2). It should be noted that due to the presence of experimental noise and shifts in real GC-MS data, only MCR-ALS and PARAFAC2 could be used for the resolution of the two analytes, phenanthrene and anthracene. PARAFAC could not be used in this case because it could not handle properly peak profiles shifts in real data. In other words, when PARAFAC was applied to these data, the resolved profiles were unreasonable and the statistical parameters were very poor. Fig. 6a shows the column-wise augmented data arrangement performed for different analyte concentration levels and Fig. 6b shows the MCR-ALS resolved elution profiles for anthracene, phenanthrene and for the baseline. LOF value was equal to 1.16 in this case.

The uncertainty associated to the measured signal (as a measure of instrumental noise) was estimated from the variance-covariance matrix of the MCR-ALS residuals, and it was equal to 9.87×10^6. From this estimation together with the resolved spectral profiles, multivariate AFOMs were calculated and reported in Table 6 for both analytes. As can be seen in Table 6, the values of LOF, slope, γ and SEL can be estimated for MCR-ALS resolved profiles. Due to the presence of experimental noise and shift, the calculated values were worse than for the previously shown simulated data.

Fig. 7 shows the resolved elution profiles of both investigated analytes using PARAFAC2. In this case, PARAFAC2 resolved reasonably well the elution profiles for the three components, phenanthrene, anthracene and baseline, in the different calibration samples. However, there were still some negative values in the resolved elution profiles which reflects PARAFAC2 impossibility of application of non-negativity constraints in the time elution mode. In addition, PARAFAC2 could not extract properly the baseline as an independent component, as MCR-ALS succeeded to do. Table 6 gives the calculated AFOMs using PARAFAC2 resolved profiles. Inspection of these results confirmed the good agreement between PARAFAC2 and MCR-ALS results in this case.

This fact that PARAFAC2 could resolve similar profiles to MCR-ALS in this experimental data case can be explained due to: (1) there were no interferences in the case of real samples, and (2) the presence of shifts and changes in the shapes of the elution profiles resulted to be rather small.

4. Concluding remarks

After analyzing the results related to the investigated hyphenated chromatographic systems, the main concluding remarks regarding the performance of three algorithms are as follows:

4.1. MCR-ALS algorithm

- When noise levels increased (0.0–1.0%), the fit to data decreased (i.e., LOF values increase). This is then reflected in the calibration figures of merit. However, no significant changes in the slope of calibration curves (calibration sensitivity) due to increasing noise levels were observed, although intercept values (offset) increased significantly. Relative prediction errors of calibration (RE) samples confirmed the effect of noise levels on the algorithm performance and calibration models.
- Increasing noise level produces poorer multivariate AFOM (except for SEL) values. However, it should be pointed out that since the SEL value depends on the amount of spectral overlapping, and these profiles were correctly resolved by MCR-ALS, final SEL values for MCR-ALS resulted to be close to unity in all cases.
- One of the clearer advantages of the MCR-ALS method is its independence from elution time shift levels. By increasing shift levels even up to a 10% of the retention time length (under the same noise level), no significant change occurred in the algorithm performance, nor in the calibration models and multivariate AFOMs.
- One of the more interesting aspects of the MCR-ALS algorithm is that it produced similar results in the absence or presence of uncalibrated species, due to the correct recovery of the analyte profiles when correct constraint is done [29].

4.2. PARAFAC algorithm

- PARAFAC results depend strongly on the amount of elution time shifts (not fulfillment of the trilinear model). By increasing the shift levels from 0 to 10% of the retention time length, the algorithm performance (LOF) decreased very significantly and very poor calibration models (considering r^2 and RE) were obtained.
- Increasing the elution time shift levels also decreased the quality of PARAFAC multivariate AFOMs. However, when elution time shifts and noise levels were low, pure component profiles could be correctly resolved, although the obtained calibration models and AFOM values resulted to be unreliable, even at the
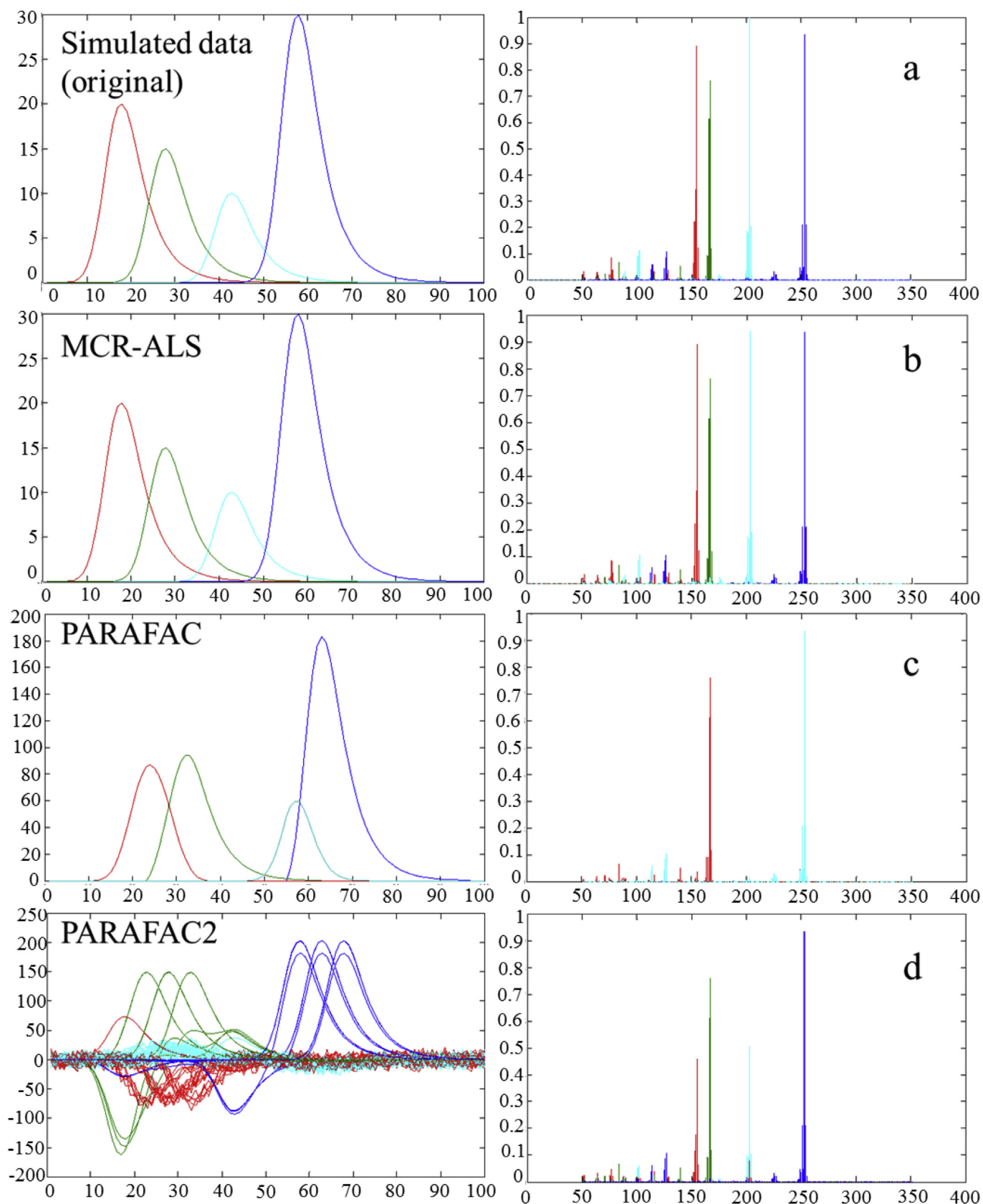
Fig. 5. Elution and spectral profiles of fluorene (green, left) and benzo[*a*]pyrene (blue, right) in (a) simulated data system (*iii*) with 5% shift and 0.1% noise level, (b) resolved by MCR-ALS, (c) resolved by PARAFAC and (d) resolved by PARAFAC2. (For interpretation of the references to colour in this figure legend, the reader is referred to the web version of this article.)
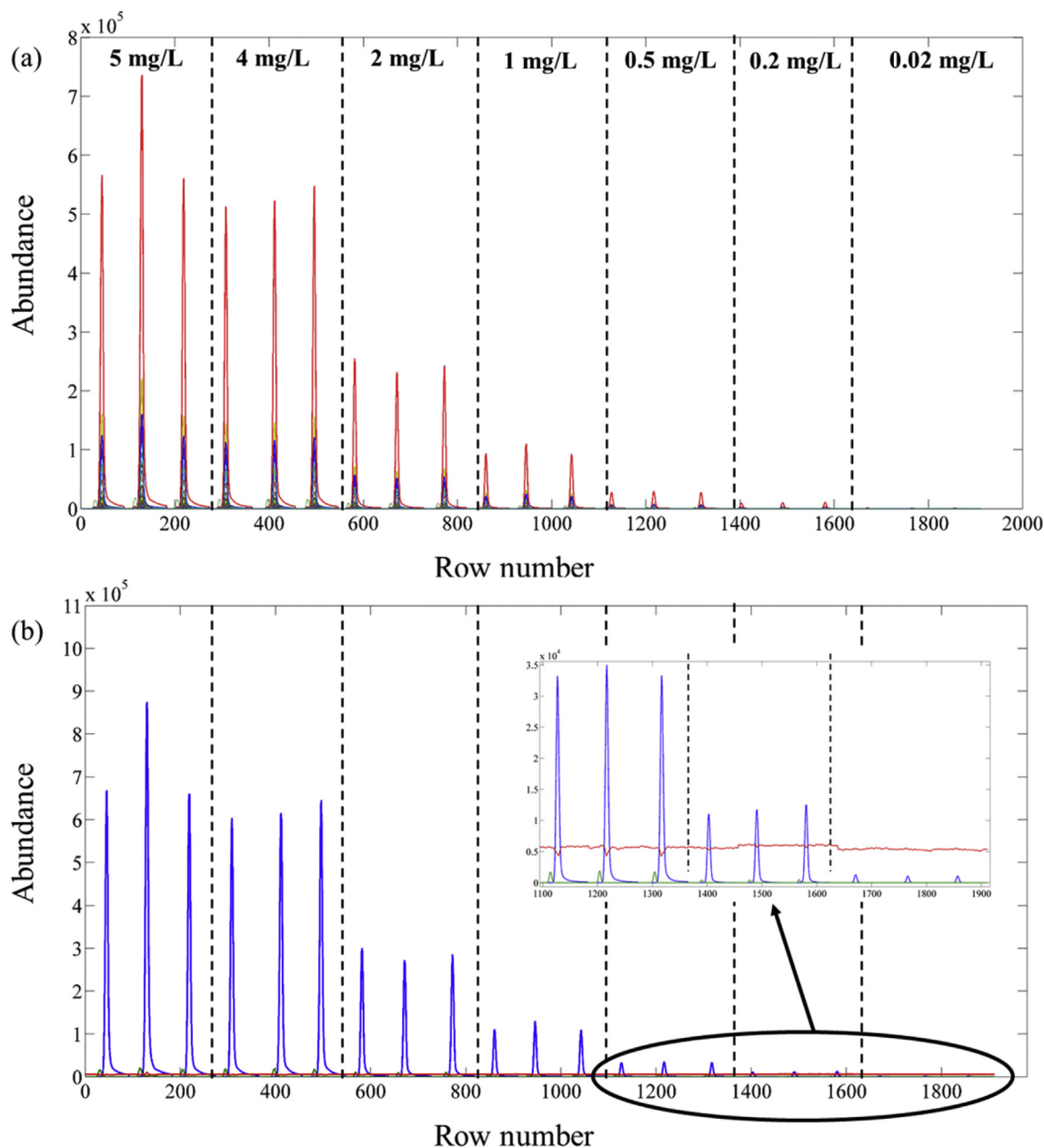
Fig. 6. (a) Augmented data matrix for GC-MS data of phenanthrene and anthracene in different concentration levels. (b) Resolved MCR-ALS elution profiles of anthracene (blue), phenanthrene (green) and baseline (red). (For interpretation of the references to colour in this figure legend, the reader is referred to the web version of this article.)

lowest shift levels (1%). When there were no elution time shifts (at all different noise levels), γ and LOD as well as LOF values were similar to those obtained for MCR-ALS.

- The performance of the PARAFAC algorithm depends also on the simultaneous absence or presence of uncalibrated species (apart from time shifts). In other words, in the presence of uncalibrated

Table 6
Calibration parameters and AFOM for anthracene and phenanthrene in real sample.

Algorithm	LOF	Slope[a]	Intercept	σx[b]	σy[c]	SEL	γ
Anthracene							
MCR-ALS	1.16	1.12×10^6	-1.28×10^{-5}	9.87×10^6	0.17	0.96	0.011
PARAFAC2	2.72	1.12×10^6	-1.43×10^{-5}	3.79×10^7	0.16	1	0.029
Phenanthrene							
MCR-ALS	1.16	2.9×10^4	2.96×10^3	9.87×10^6	0.09	0.94	2.9×10^{-4}
PARAFAC2	2.72	1.45×10^4	4.74×10^5	3.79×10^7	0.94	1	3.8×10^{-4}

[a] Slope of pseudo-univariate calibration curve.
[b] Uncertainty in signal.
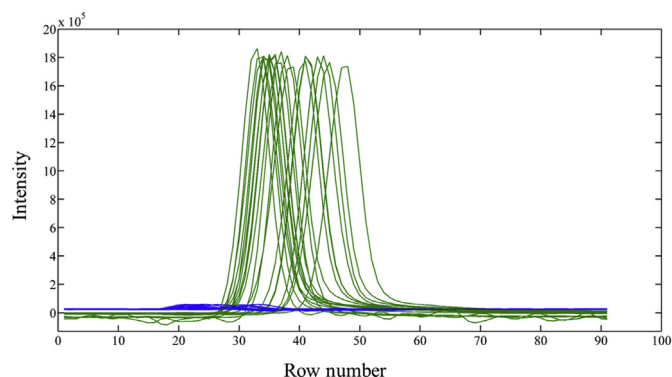[c] Uncertainty in predicted concentration.

Fig. 7. Resolved PARAFAC2 elution profiles of anthracene (green) and phenanthrene (blue). (For interpretation of the references to colour in this figure legend, the reader is referred to the web version of this article.)

species in the test set, the multivariate AFOMs were worse than when they were absent.

4.3. PARAFAC2 algorithm

- PARAFAC2 results were strongly dependent on the noise level and on the elution time shift pattern. PARAFAC2 could not resolve properly the components in the simultaneous presence of noise and time shifts in the case of simulated data systems (*i*) and (*ii*). In some cases, the number of iterations was very large (more than 10,000 with stopping criterion 1×10^{-5}), and no proper resolution was achieved yet. In the case of noiseless data and with shift levels of 0–10%, PARAFAC2 gave better LOF values compared to PARAFAC, thus providing better AFOMs.

- PARAFAC2 could handle up to 10% random elution time peak shifts in the data in calibrated-two-component system, but only in the case of noiseless data. PARAFAC2 results were unreliable when noise was present in the analyzed data. In the presence of noise, PARAFAC2 did not give reasonable calibration models and consequently, multivariate AFOM were not good either. Rather low SEL and γ values and large LODs confirmed the poorer performance of PARAFAC2 in the resolution of different systems with different chromatographic complexities and artifacts.

Appendix A. Supplementary data

Supplementary data related to this article can be found at http://dx.doi.org/10.1016/j.aca.2016.11.070.

References

[1] L.A. Currie, Nomenclature in evaluation of analytical methods, including detect ion and quantification capabilities (IUPAC technical report), Pure Appl. Chem. 67 (1995) 1699–1723.
[2] L.A. Currie, Detection and quantification limits: origins and historical overview, Anal. Chim. Acta 391 (1999) 127–134.
[3] G.M. Escandar, A.C. Olivieri, N.K.M. Faber, H.C. Goicoechea, A.M. de la Peña, R.J. Poppi, Second- and third-order multivariate calibration: data, algorithms and applications, Trends Anal. Chem. 26 (2007) 752–765.
[4] A.C. Olivieri, Recent advances in analytical calibration with multi-way data, Anal. Methods 4 (2012) 1876–1886.
[5] A. Lorber, K. Faber, B.R. Kowalski, Net analyte signal calculation in multivariate calibration, Anal. Chem. 69 (1997) 1620–1626.
[6] J. Ferré, N. (Klaas), M. Faber, Net analyte signal calculation for multivariate calibration, Chemom. Intell. Lab. Syst. 69 (2003) 123–136.
[7] C.N. Ho, G.D. Christian, E.R. Davidson, Application of the method of rank annihilation to fluorescent multicomponent mixtures of polynuclear aromatic hydrocarbons, Anal. Chem. 52 (1980) 1071–1079.
[8] N.J. Messick, J.H. Kalivas, P.M. Lang, Selectivity and related measures for nth-

[9] A.C. Olivieri, N.M. Faber, Standard error of prediction in parallel factor analysis of three-way data, Chemom. Intell. Lab. Syst. 70 (2004) 75–82.
[10] A.C. Olivieri, K. Faber, New developments for the sensitivity estimation in four-way calibration with the quadrilinear parallel factor model, Anal. Chem. 84 (2011) 186–193.
[11] F. Allegrini, A.C. Olivieri, Analytical figures of merit for partial least-squares coupled to residual multilinearization, Anal. Chem. 84 (2012) 10823–10830.
[12] C. Bauza, G.A. Iban, R. Tauler, A.C. Olivieri, Sensitivity equation for quantitative analysis with multivariate curve resolution-alternating least-squares: theoretical and experimental approach, Anal. Chem. 84 (2012) 8697–8706.
[13] A.C. Olivieri, Analytical figures of merit: from univariate to multiway calibration, Chem. Rev. 114 (2014) 5358–5378.
[14] R.M. Maggio, M.A. Rivero, T.S. Kaufman, Journal of Pharmaceutical and Biomedical Analysis Simultaneous acquisition of the dissolution curves of two active ingredients in a binary pharmaceutical association, employing an on-line circulation system and, J. Pharm. Biomed. Anal. 72 (2013) 51–58.
[15] M.R. Alcaráz, L. Vera-candioti, M.J. Culzoni, H.C. Goicoechea, Ultrafast quantitation of six quinolones in water samples by second-order capillary electrophoresis data modeling with multivariate curve resolution-alternating least squares, Anal. Bioanal. Chem. 406 (2014) 2571–2580.
[16] R.L. Pérez, G.M. Escandar, Solid-surface fluorescent properties of estrogens: green analytical applications, Microchem. J. 118 (2015) 141–149.
[17] M.R. Alcaráz, A.V. Schenone, M.J. Culzoni, H.C. Goicoechea, Modeling of second-order spectrophotometric data generated by a pH-gradient fl ow injection technique for the determination of doxorubicin in human plasma, Microchem. J. 112 (2014) 25–33.
[18] R.L. Pérez, G.M. Escandar, Liquid chromatography with diode array detection and multivariate curve resolution for the selective and sensitive quanti fi cation of estrogens in natural waters, Anal. Chim. Acta 835 (2014) 19–28.
[19] H. Parastar, R. Tauler, Multivariate chemometric resolution of hyphenated and multidimensional chromatographic measurements: a new insight to address current chromatographic challenges, Anal. Chem. 86 (2014) 286–297.
[20] M. Jalali-Heravi, H. Parastar, Assessment of the co-elution problem in gas chromatography-mass spectrometry using non-linear optimization techniques, Chemom. Intell. Lab. Syst. 101 (2010) 1–13.
[21] C.B. Zachariassen, J. Larsen, F. van den Berg, R. Bro, A. de Juan, R. Tauler, Comparison of PARAFAC2 and MCR-ALS for resolution of an analytical liquid dilution system, Chemom. Intell. Lab. Syst. 83 (2006) 13–25.
[22] M.V. Bosco, M.S. Larrechi, PARAFAC and MCR-ALS applied to the quantitative monitoring of the photodegradation process of polycyclic aromatic hydrocarbons using three-dimensional excitation emission fluorescent spectra Comparative results with HPLC, Talanta 71 (2007) 1703–1709.
[23] S.A. Bortolato, J.A. Arancibia, G.M. Escandar, Non-trilinear chromatographic time retention-fluorescence emission data coupled to chemometric algorithms for the simultaneous determination of 10 polycyclic aromatic hydrocarbons in the presence of interferences, Anal. Chem. 81 (2009) 8074–8084.
[24] S.A. Bortolato, A.C. Olivieri, Chemometric processing of second-order liquid chromatographic data with UV − vis and fl uorescence detection. A comparison of multivariate curve resolution and parallel factor analysis 2, Anal. Chim. Acta 842 (2014) 11–19.
[25] Y. Kalambet, Y. Kozmin, K. Mikhailova, I. Nagaev, P. Tikhonov, Reconstruction of chromatographic peaks using the exponentially modified Gaussian function, J. Chemom. 25 (2011) 352–356.
[26] T.G. Bloemberg, J. Gerretzen, A. Lunshof, R. Wehrens, L.M.C. Buydens, Warping methods for spectroscopic and chromatographic signal alignment: a tutorial, Anal. Chim. Acta 781 (2013) 14–32.
[27] H. Parastar, N. Akvan, Multivariate curve resolution based chromatographic peak alignment combined with parallel factor analysis to exploit second-order advantage in complex chromatographic measurements, Anal. Chim. Acta 816 (2014) 18–27.
[28] R. Bro, PARAFAC. Tutorial and applications, Chemom. Intell. Lab. Syst. 38 (1997) 149–171.
[29] R. Tauler, Multivariate curve resolution applied to second order data, Chemom. Intell. Lab. Syst. 30 (1995) 133–146.
[30] R. Bro, C.A. Andersson, H.A.L. Kiers, PARAFAC2-Part II. Modeling chromatographic data with retention time shifts, J. Chemom. 13 (1999) 295–309.
[31] C.R. Rao, S. Mitra, Generalized Inverse of Matrices and its Applications, Wiley, New York, 1971.
[32] A. smilde, R. Bro, P. Geladi, Multi-way Analysis with Applications in the Chemical Sciences, Wiley, Chichester, 2004.
[33] P.D. Wentzell, Measurement errors in multivariate chemical data, J. Braz. Chem. Soc. 25 (2014) 183–196.
[34] A.C. Olivieri, N.M.K.M. Faber, J. Ferré, R. Boqué, J.H. Kalivas, H. Mark, Uncertainty estimation and figures of merit for multivariate calibration (IUPAC Technical Report), Pure Appl. Chem. 78 (2006) 633–661.
[35] NIST/epa/NIH MS Library, 2005 v. 2.0d, Gaithersburg, MD, USA.
[36] MCR-ALS homepage at www.mcrals.info, Accessed 01 February 2016.
[37] C.A. Andersson, R. Bro, N-way toolbox for MATLAB, Chemom. Intell. Lab. Syst. 52 (2000) 1–4.
[38] W. Windig, J. Guilment, Interactive self-modeling mixture analysis, Anal. Chem. 63 (1991) 1425–1432.